Protein Engineering vol. 16 no. 12 pp. 993–1003, 2003
DOI: 10.1093/protein/gzg122

Structure–function discrimination of the N- and C- catalytic domains of human angiotensin-converting enzyme: implications for Cl^- activation and peptide hydrolysis mechanisms

Andreas G.Tzakos[1], Athanassios S.Galanis[2], Georgios A.Spyroulias[2], Paul Cordopatis[2], Evy Manessi-Zoupa[3] and Ioannis P.Gerothanassis[1,4]

[1]Department of Chemistry, University of Ioannina, GR-45110 Ioannina and Departments of [2]Pharmacy and [3]Chemistry, University of Patras, GR-26504 Patras, Greece

[4]To whom correspondence should be addressed.
E-mail: igeroth@cc.uoi.gr

Human somatic angiotensin I-converting enzyme (*s*ACE) has two active sites present in two sequence homologous protein domains (ACE_N and ACE_C) possessing several biochemical features that differentiate the two active sites (i.e. chloride ion activation). Based on the recently solved X-ray structure of testis angiotensin-converting enzyme (*t*ACE), the 3D structure of ACE_N was modeled. Electrostatic potential calculations reveal that the ACE_N binding groove is significantly more positively charged than the ACE_C, which provides a first rationalization for their functional discrimination. The chloride ion pore for Cl2 (one of the two chloride ions revealed in the X-ray structure of *t*ACE) that connects the external solution with the inner part of the protein was identified on the basis of an extended network of water molecules. Comparison of ACE_C with the X-ray structure of the prokaryotic ClC Cl^- channel from *Salmonella enterica* serovar *typhimurium* demonstrates a common molecular basis of anion selectivity. The critical role for Cl2 as an ionic switch is emphasized. Sequence and structural comparison between ACE_N and ACE_C and of other proteins of the gluzincin family highlights key residues that could be responsible for the peptide hydrolysis mechanism. Currently available mutational and substrate hydrolysis data for both domains are evaluated and are consistent with the predicted model.

Keywords: angiotensin I-converting enzyme/catalytic mechanism/chloride ion activation/gluzincins/homology modelling

Introduction

Mammalian angiotensin I-converting enzyme (ACE) (peptidyl dipeptidase A, kininase II, EC 3.4.15.1) is a zinc dipeptidyl carboxypeptidase (Corvol *et al*., 1995; Corvol and Williams, 1996) responsible for the conversion of angiotensin I to the powerful vasoconstrictor angiotensin II (Tzakos *et al*., 2003) and the inactivation of the vasodilatory peptide bradykinin by the removal of C-terminal dipeptides (Erdos, 1990). Reports of the existence of ACE-like proteins in several insects, a crab, a tick, an annelid and a mollusc have established that ACE is an evolutionarily ancient enzyme (Coates *et al*., 2000). ACE is expressed as a somatic isoform (*s*ACE, 150–180 kDa) in endothelial, epithelial and neuroepithelial cells and as a smaller isoform (*t*ACE, 90–110 kDa) only in male germinal cells. Both isoforms are primarily plasma membrane enzymes, anchored by a common C-terminal hydrophobic region. Human somatic ACE is a two-domain protein resulting from a tandem gene duplication (Hubert *et al*., 1991; Soubrier *et al*., 1993a,b; Williams *et al*., 1994), with each domain possessing dipeptidyl carboxypeptidase activity and distinctive substrate specificity (Wei *et al*., 1991, 1992). It consists of two homologous, zinc catalytic domains of ~600 residues each [called N- (ACE_N) and C- (ACE_C) terminal, respectively], with slightly different catalytic activities; a juxtamembrane 'stalk' region, a transmembrane hydrophobic sequence and a 30 residue, C-terminal cytosolic domain. The germinal form of ACE contains a single active site and corresponds to the C-domain of the somatic enzyme (Corvol *et al*., 1995; Azizi *et al*., 1996; Corvol and Williams, 1996; Hagaman *et al*., 1998). Because of its central role in the metabolism of vasoactive peptides, ACE has attracted intense interest for the development of orally active ACE inhibitors to treat hypertension and because the ACE gene is a candidate gene for several cardiovascular diseases (Soubrier *et al*., 1993a,b). Recently, an ACE homologue, referred to as ACE2, was identified in humans and shown to be an essential regulator of cardiac function (Donoghue *et al*., 2000; Tipnis *et al*., 2000). It differs from classical ACE in being a carboxypeptidase that preferentially removes C-terminal hydrophobic or basic amino acids and is not affected by ACE inhibitors.

The primary activity of ACE is to cleave free carboxyl group oligopeptides with a wide specificity (Rohrbach *et al*., 1981). Substrates containing Pro at the P1′ position [nomenclature by Schechter and Berger (Schechter and Berger, 1967)] and Asp or Glu at P2′ are resistant to ACE. However, ACE can also work as an endopeptidase or a tripeptidyl carboxypeptidase upon certain substrates. The endopeptidase activity of ACE is observed with substrates that have amidated carboxyl groups where the enzyme can cleave a C-terminal dipeptide amide and/or a C-terminal tripeptide amide (Erdos, 1990; Hooper, 1991). ACE can cleave luteinizing hormone-releasing hormone (LH-RH) not only at the C-terminal tripeptide amide but also at the N-terminal tripeptide (Skidgel and Erdos, 1985).

The C- and N-domains of the somatic form of ACE (Wei *et al*., 1991) exhibit similar catalytic activities towards angiotensin I, bradykinin and substance P (Jaspard *et al*., 1993). However, the activity of the C-terminal domain is highly dependent on chloride ion concentration, whereas the N-terminal domain is still active in the absence of chloride and is fully activated at relatively low concentrations of this anion (Wei *et al*., 1991; Jaspard *et al*., 1993). The N active site is preferentially involved in the N-terminal endopeptidase cleavage of LH-RH, but with low catalytic efficiency (Jaspard *et al*., 1993). Captopril, lisinopril and RXP-407 display different inhibitory potencies towards the two active sites (Ehlers and Riordan, 1991; Wei *et al*., 1992; Dive *et al*., 1999). In addition to the well-known function of ACE in the renin–angiotensin

system, it has been demonstrated that the N active site of the enzyme hydrolyses the natural circulating tetrapeptide *N*-acetyl-L-seryl-L-aspartyl-L-lysyl-2-proline (Ac-SDKP), which is involved in the control of hematopoietic stem cell proliferation (Rousseau *et al*., 1995). The demonstration that the physiological functions of ACE are not limited to its cardiovascular role and that the enzyme degrades Ac-SDKP both *in vivo* and *in vitro* (Rieger *et al*., 1993; Rousseau *et al*., 1995; Azizi *et al*., 1996) increased interest in studies of each domain specificity and inhibition (Dive *et al*., 1999; Michaud *et al*., 1997, 1999). Another specific substrate for the N-domain is angiotensin 1–7 (D-R-V-Y-I-H-P) but at the same time this peptide inhibits the hydrolysis of angiotensin I by the C-domain (Deddish *et al*., 1998).

Recently, the crystal structures of *t*ACE at 2.0 Å resolution (Natesh *et al*., 2003) and of *Drosophila* ACE (Taylor *et al*., 1996) at 2.4 Å resolution (Kim *et al*., 2003) have been determined. The enzyme has a deep, narrow channel that runs the length of the molecule and the active site is located about midway along the floor of this channel. Based on the high degree of sequence identity between the *t*ACE and the N-catalytic domain of *s*ACE (ACE_N), we present here the three-dimensional structure of the ACE_N and the identification of sequence differences that may contribute to the differential cleavage site recognition in the two domains of the enzyme. Because relatively few sequence differences can be identified near the active site region, we can assess the significance of these changes for substrate recognition. The locations of critical residues conserved in the overall family have been identified and are discussed in terms, first, of the currently available mutational and substrate hydrolysis data, secondly, on the structural basis of the different activation profiles of ACE_C and ACE_N in the presence of chloride ions, and thirdly, in the framework of a common peptide–substrate hydrolysis mechanism (Matthews, 1988).

Materials and methods

The amino acid sequences used in the present studies were retrieved from the SWISSPROT database (Bairoch and Apweiler, 2000). Multiple sequence alignment was accomplished employing CLUSTALW (Thompson *et al*., 1994). Sequence-to-structure alignments were obtained using the TopLign fold recognition method (Thiele *et al*., 1999). Coordinate files of template proteins were downloaded from the Protein Data Bank (Berman *et al*., 2000). Structural neighbour searching and comparison were performed with DALI (Holm and Sander, 1993), FSSP (Holm and Sander, 1996), SCOP (Murzin *et al*., 1995), VAST (Gibrat *et al*., 1996) and CATH (Orengo *et al*., 1997).

The structure of ACE_N (20 models) was constructed through comparative modelling by using MODELER v6.1 (Sali *et al*., 1995) based on the recently solved crystal structure of the ACE_C domain (PDB i.d.: 1O8A) (Natesh *et al*., 2003). From the 20 models, the one having the lowest energy (Sippl, 1993) and best stereochemistry was selected (Laskowski *et al*., 1993). The root mean square deviation of all backbone atoms was found to be 0.19 Å for the native ACE_C and 0.26 Å for the ACE_C–lisinopril complex, with no changes in secondary assignments. We then used two protein structure verification methods that characterize the environments of residues to assess the ACE_N model relative to the X-ray ACE_C structure. Both the PROFILER3D (Luthy *et al*., 1992) and ERRAT (Colovos and Yeates, 1993) programs gave comparable scores for ACE_N and ACE_C. Identification of cavities in ACE_C was performed with CASTp (Liang *et al*., 1998). Electrostatic potential maps were calculated with MOLMOL (Koradi *et al*., 1996).

Results and discussion

Mapping residue sequence, structure and charge surface differences of ACE_N and ACE_C—comparison with substrate hydrolysis and mutational data

Recently, Chubb *et al*. suggested, as boundaries of the *g*ACE ectodomain, D40 at the N-terminus and G615 at the C-terminus, corresponding to D641 and G1241 of the C-terminal catalytic site of *s*ACE (Chubb *et al*., 2002).

The repeated region of the somatic ACE possesses the two characteristic gluzincin HEXXH and EXXXD motifs separated by a 23-residue spacer (Soubrier *et al*., 1988; Wei *et al*., 1991). The HEXXH sequence is a common motif found in numerous metalloproteases, including the thermolysin family, astacin, deformylase and the M1 aminopeptidases. It has been proposed (Soubrier *et al*., 1988; Hooper, 1994) that the two histidine residues in the former sequence are two of the four zinc ligands, and the third ligand is the glutamate residue of the latter sequence as assigned by the X-ray structure (Natesh *et al*., 2003). A feature characterizing the sequence of *s*ACE is the high number of proline residues. In both the C- and N- catalytic domains of the *s*ACE sequence, two proline residues are located in the 23-residue spacer.

In the repeated regions 10 cysteine residues are contained. Three adjacent disulfide linkages (*aabbcc*) with a free cysteine positioned between the C-terminal part and the middle disulfide bonds have been identified in *t*ACE (Sturrock *et al*., 1996) and confirmed by the X-ray structure of *t*ACE. These are Cys152–Cys158 (a), Cys352–Cys370 (b) and Cys538–Cys550 (c), whilst Cys496 (d) was identified as the only unpaired. In the N-terminal part of *s*ACE, the relevant disulfide linkages represent Cys359–Cys377 (b), Cys545–Cys557 (c) and Cys503 is the unpaired residue (e). In the C-terminal part of *s*ACE the relevant disulfide linkages represent Cys957–Cys975 (b), Cys1143–Cys1155 (c) and Cys1101 (e) corresponds to Cys496 of *g*ACE. The Cys152–Cys158 (a) of *g*ACE corresponds to Cys757-Cys763 of the *s*ACE located in the intermediate region between the N- and C- repeated regions.

The amino acid sequence alignment of the ACE_C and ACE_N catalytic domains differ in length by seven residues [shown in Figure S1 (available as supplementary material at http://protein.oupjournals.org); for sequence numbering of ACE_C, we have used the numbering followed in *t*ACE]. Sequence homology among the two enzyme domains is ~55%. The differences in primary sequence are well distributed over the length of the two proteins. Superposition of the homology modelled structure of ACE_N with the X-ray structure of the native *t*ACE (ACE_C) gave an r.m.s.d. of 0.19 Å (supplementary Figure S2). Using the crystal structure of ACE_C (Natesh *et al*., 2003), we have determined residues at the molecular surface, which differ from the corresponding residues in ACE_N.

In the substrate-binding channel the majority of the sequence differences are located in non-α-helical or β-sheet areas (denoted with white lines in supplementary Figure S1). The gluzincin motif $HEMGHX_{23}E$ is located on the floor of the channel, which is represented by residues 373–393 (helix),

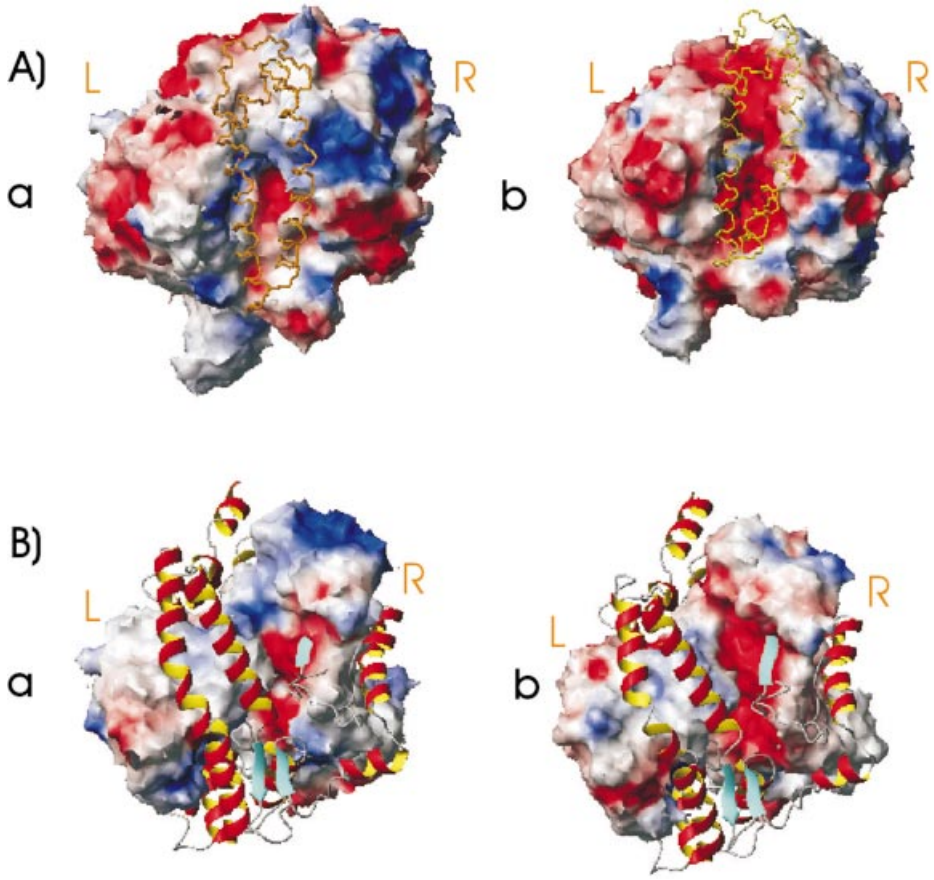

Fig. 1. (**A**) View of the surface potential of ACE_N (a) and ACE_C (b) (negative and positive potentials in red and blue, respectively). (**B**) Cutaway views of the substrate-binding channels for ACE_N (a) and ACE_C (b). The right and left 'walls' of the substrate-binding groove are denoted R and L respectively (in orange).

405–423 and 521–538. The changes R381/E403, L370/M392 and S378/A400 (the ACE_N residue is listed first) occur in residues close to the cleavage site that potentially could interact with the bound substrate. Other changes mapped on the floor of the binding groove are G439/S461 near the pyrrolidinic ring of lisinopril and R340/G362, distant from the lisinopril-binding groove.

The walls of the binding site are formed by residues 350–372 (antiparallel strand) and 456–519, the edges by 394–404 and 424–433 and the lip by residues 40–130. On the right (R) wall (R, Figure 1), near the region of the lysyl group of lisinopril, the aliphatic changes V359/A381 and polar–apolar changes T358/V384 and S357/V379 can be seen. An interesting positive to negative charge alternation Q355/D377 is observed before the gluzincin-binding motif. On the top of the right wall (R) the changes R350/T372 and T352/N374 can be seen. On the left (L) wall of the binding groove (L, Figure 1), the changes N494/S516, S529/V483 and T496/V518 can be observed near the pocket where the phenyl ring of lisinopril is located. On the top of this wall the alterations T478/P500, N470/T502, E481/Q503, T482/G504, H483/D505 and A486/P508 (near the Cl^-) can be observed.

Substrate peptides are expected to extend largely along the channel floor and the walls. In order to assign further potent functional differentiations of the binding grooves of the two domains, the surface potentials of the lisinopril-binding groove (floor and walls) were computed for both the ACE_C and ACE_N (Figure 1B). The results indicate a profound difference in the charged surfaces between the two binding grooves: the ACE_N binding groove appears more positively charged than the ACE_C. This is a first clue indicating functional differentiation of substrate recognition and binding of the two domains of sACE from a structural point of view. Differences in charge density distribution were also observed in the case of the lips (helixes α1 and α2) of ACE_N and ACE_C (data not shown; available as supplementary Figure S3). Specifically, the lip of the ACE_N domain (residues 13–96) appears more negatively charged than the lip of the ACE_C domain (residues 40–120), both near the gluzincin motif $HEMGHX_{23}E$ (inside the binding groove) and in the outer, exposed, part.

ACE inhibitors bind to both active sites but, depending on their structure, they may differ in their affinities, primarily because of differences in dissociation rates from the two active sites (Wei *et al*., 1992; Perich *et al*., 1994; Deddish *et al*., 1996). Functional discrimination of the two domains of ACE_C and ACE_N could be rationalized on the differences of the S1 and S1′ pockets. Specifically, the residues S516, S517 and V518 of the S1 and D377, V379, V380 and A390 of the S1′ pocket of ACE_C are altered to N494, V495 and T496 of the S1 and to Q355, S357, T358 and V359 of the S1′ pocket of ACE_N. Lisinopril and enalaprilat bind to human sACE with K_i 0.39 and 0.65 nM, respectively. Lisinopril and enalaprilat inhibit preferentially the C-domain more than the N-domain, at high chloride concentration (300 mM Cl^-); the K_i values for

these inhibitors were found to be about 18- and 4-fold lower for the C-domain than the N-domain, respectively. However, at low chloride concentration (20 mM Cl^-), enalaprilat inhibits preferentially the N-domain, since K_i is 2-fold lower for the N-domain, whereas lisinopril still inhibits the C-domain, as K_i is about 1.6-fold lower for this domain (Wei *et al*., 1991). In ACE_C the lysine side chain of lisinopril forms a salt bridge with D377, whereas in ACE_N in the same position is located Q355. This salt bridge could rationalize the fact that replacement of lysine in lisinopril by alanine in enalaprilat results in reduced binding for the C-domain, but increased binding for the N-domain. In addition, the E162/D140 alteration in ACE_N (ACE_C/ACE_N) has as a result an increment in the distance between the side chain of D140(OE2) and the lysine side chain (NH_2) of lisinipril, suggesting a lower affinity of ACE_N for lisinopril compared with that of ACE_C.

Hydrolysis of bradykinin is favoured in ACE_N (Jaspard *et al*., 1993) having F in P1 and S in P1′ positions due to possible amino–aromatic interactions of F with N494 of S1 and potent hydrogen bonding interactions of S with S357, T358 of S1′ of ACE_N. Similarly, the hydrolysis of Abz-SDK(Dnp)P-OH is also favoured by ACE_N, but not in ACE_C and this could be rationalized through electrostatic interactions of D (P1) with N494 (S1) and K (P1′) with Q385 (S1′). Further investigations of bradykinin-related peptides revealed that Abz-GFSPFFQ-EDDnp (having F in P1 and Q in P1′ positions) was preferentially hydrolysed by the C-domain, whereas Abz-GFSPFQQ-EDDnp (having Q in both the P1 and P1′ positions) exhibits higher N-domain specificity (Araujo *et al*., 2000). This differentiation could be attributed to electrostatic interactions of Q (P1) of the substrate Abz-GFSPFQQ-EDDnp with N494 in S1 of ACE_N (S516 in ACE_C), whereas in the case of the substrate Abz-GFSPFFQ-EDDnp, F (P1) could be stabilized through hydrophobic interactions with V518 in S1 (T496 in ACE_N). As shown in the X-ray structure, Y200 (F178 in ACE_N) is hydrogen bonded to S517 (V495 in ACE_N) of the S1 and contributes to the organization of this binding pocket. Mutation of this residue to F in *t*ACE (Chen *et al*., 1992; Sen *et al*., 1993) resulted in a marked decrease in the catalytic activity of the enzyme due to disruption of such interactions in ACE_C and modification of the S1 binding pocket. In ACE_N, F178 is located in position Y200 of ACE_C that forms hydrophobic interactions with V495 (S517 in ACE_C). Hence we would expect that a similar F178 to Y mutation in ACE_N would not affect significantly its catalytic activity.

A key question that could be addressed is the mechanism of the mixed-type inhibition mode of several synthetic inhibitors (Goli and Galardi, 1986; Ucar and Ozer, 1992; Baudin and Benetau-Burnat, 1999). Cotton *et al*. constructed a series of bradykinin-potentiating peptides (BPP) and found them to be selective inhibitors for the C-domain of ACE (Cotton *et al*., 2002). The most selective inhibitor of the C-domain of ACE was found to be BPPb, having lysine and proline in positions P1′ and P2′, respectively (like lisinopril). Instead, the BPPc inhibitor having proline both in P1′ and P2′ positions displayed a mixed inhibition mode, which could be ascribed to the presence of conformational isomerization of the proline in position P1′. Furthermore, as discussed above, in enalaprilat, which inhibits basically ACE_N, in P2′ is located a proline and in P1′ is located an alanine. In lysinopril, an ACE_C inhibitor, in P2′ is located a proline (accommodated by the same interactions of the S2′ subsite of ACE_C/ACE_N through hydrophobic interaction with the aromatic ring of Y523/489 and by the hydrophobic pocket formed by aromatic rings of Y520/486, F457/423 and F527/493) and in P1′ a lysine (accommodated by different interactions of the S1′ subsite of ACE_C/ACE_N through E162/D140 and D377/Q355). Hence the residue located in position P1′ of the inhibitor could be characterized as the basic driving force for inhibitor selectivity for the N- and C-domains, owing to specific differences in the S1′ subsite in the two domains.

Finally, it should be noted that *in vitro* studies indicated that full inhibition of the AI and BK cleavage requires a blockade of the two ACE active sites. In contrast, *in vivo* experiments in mice demonstrated that the selective inhibition of either the N-domain or the C-domain of ACE by these inhibitors prevents the conversion of AI to AII, whereas BK protection requires the inhibition of the two ACE active sites (Georgiadis *et al*., 2003). This rules out the scenario that *in vivo* the binding of the inhibitor of one site produces the inactivation of the other active site, free of inhibitor (Kost *et al*., 1998). It should be kept in mind that *in vitro* experiments are based on a soluble form of *s*ACE, whereas the *in vivo* experiments are dependent on ACE in its membrane-bound form. Taken together, these studies indicate that the membrane-bound form of ACE may control some physiological functions of ACE. Hence *in vitro* experiments based on soluble forms of ACE may not properly reflect the function of ACE in its membrane environment. Therefore, it is imperative to understand the topology of ACE on the cell membrane. Kost *et al*. have examined the structure of ACE in reverse micelles (biomembrane modelling system) and found that somatic ACE forms dimers via carbohydrate-mediated interaction, providing evidence for the existence of a carbohydrate-recognizing domain localized on the N-domain of the ACE molecule (Kost *et al*., 2003). Previously, the same group demonstrated that bovine somatic ACE can be detected in reverse micelles not only as a monomer but also as a homodimer (Kost *et al*., 1994, 1998; Grinstein *et al*., 1999) and that ACE can function in different oligomeric forms in an artificial membrane with dimers and tetramers being more catalytically active than ACE monomers (Grinstein *et al*., 1999, 2001). The recently solved structure of the testis isoform of human ACE and that of *Drosophila* clearly have shed light and opened new horizons for the elucidation of the structural biology of this polysynthetic and possibly multifunctional enzyme. Nevertheless, crucial questions about the precise arrangement of the two domains and the nature of the interaction between their respective active sites (antagonistic or in a synergistic manner for substrate selection) and the structure organization of *s*ACE within the cell membrane architecture remain.

The structural and functional role of the chloride ions of ACE_N and ACE_C. Comparison with substrate hydrolysis and mutational data and the X-ray structure of StCLC selectivity filters

Substrate hydrolysis by ACE is activated by chloride ions in a substrate-dependent manner (Bunning and Riordan, 1983; Shapiro *et al*., 1983). This feature is unique among metalloproteases; however, the molecular mechanism of this regulation is unclear. For example, the degree of enzyme activation by Cl^- and its apparent dissociation constant ($K_{d,\ app}$) associated with this activation is high for angiotensin I and low for bradykinin (Bunning and Riordan, 1983; Shapiro *et al*., 1983). The hydrolysis of Abz-peptidyl-EDDnp peptides indicates a higher dependence to Cl^- compared with Abz-peptidyl-

Table I. Amino acid residues of ACE_C and ACE_N that might be implicated in the binding mode of the chloride ions Cl1 and Cl2 and their respective shortest distances in Å

Cl1		Distance (Å)	Cl2		Distance (Å)
ACE_C	ACE_N		ACE_C	ACE_N	
R186(NE) (+)[a]	H164	3.2	Y224(OH)	Y202	3.0
R489(NH1)	R467	3.2	R522(NE)	R500	3.1
W485(NE1)	W463	3.3	P407(CB)	P385	3.6
W486(CZ2)	W464	3.5	P519(CB)	P497	3.6
W279(CD1)	W257	5.2	I521(CG2)	I499	3.6
D507(CB)	D485	3.8	M223(CE)	W201	4.0
			W220(C)	W198	6.0

[a](+) indicates the presence of a destabilizing hydrophobic–hydrophilic contact.

Table II. Amino acid residue differences between ACE_C and ACE_N that might be significant for the binding of lisinopril and their respective distances in Å

Lisinopril[a]		Distance (Å)
ACE_C	ACE_N	
E162(OE2)	D140	3.5
V518(CG2)	T496	3.8
V380(CG2)	T358	3.9(+)[b]
D377(OD1)	Q355	4.2
#R522(NH1)	#R500	5.1
E376(OE2)	D354	5.5
S516(CB)	N494	5.7
N70(OD1)	D43	5.8
E143(OE1)	S119	5.8
*W279(CZ3)	*W257	6.4
N66(ND2)	S39	6.4

[a]Symbols * and # denote residues with common contacts to both lisinopril and Cl1/Cl2, respectively.
[b](+) indicates the presence of a destabilizing hydrophobic–hydrophilic contact.

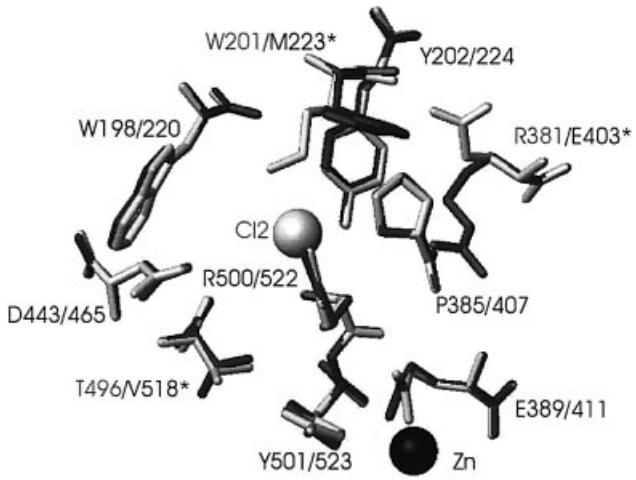

Fig. 2. The binding site of Cl2 in ACE_C (white) and ACE_N (grey) (the ACE_N numbering first). Amino acid differences of ACE_N are indicated with asterisks.

K(Dnp)P-OH substrates. It was suggested that the absence of a negative charge of the C-terminal carboxyl group is compensated by chloride ion (Araujo *et al*., 2000) and that disruption of an electrostatic interaction between the C-terminal carboxyl group of the substrate Abz-GFSPFRA-EDDnp and a basic group of the enzyme at pH > 8.0 reduces the hydrolysis of the substrate containing a free carboxyl group.

The crystal structure of *t*ACE (ACE_C) revealed the location of two buried chloride ions separated by 20.3 Å. The first (Cl1) is found 20.7 Å and the second (Cl2) 10.4 Å away from the zinc ion. The Cl1 binding residues W279 of ACE_C and W257 of ACE_N are also common binding sites for the substrate–lisinopril in the wall of the binding groove (Tables I and II). Cl1 is very close to K511 (K489 of ACE_N) that stabilizes the C-terminal carboxylate group of lisinopril. Interestingly, the carboxylate group of N-carboxylalanine (NXA) of the native protein is fully superimposed on the C-terminal carboxylate group of lisinopril (PDB i.d.: 1O8A). Hence it could be suggested that Cl1 is the synergistic anion of importance for high-affinity substrate binding through structural orientation of K511. Specifically, in the absence of the chloride ion, K511 could form amino–aromatic interactions with W279, W485 and W486 (K489 of ACE_N with W257, W463 and W464) (Scrutton and Raine, 1996). As a result of these interactions, the positive charge of the side chain is not available for stabilization of the C-terminal carboxylate group of the substrate.

The second chloride ion (Cl2) could be the mechanistically significant anion binding (MESAB) similar to the kinetically significant anion binding (KISAB) in human transferrin (He *et al*., 2000). Cl2 is bound to R522 that has been reported to be critical for the chloride dependence of ACE activity (Liu *et al*., 2001). The molecular mechanism of chloride activation is not readily apparent from the structure; however, the primary ligand for Cl2, R522, lies on the same helix (α17) as Y520 and Y523 which interact with lisinopril and, presumably, also the substrate.

In Table I, we have mapped the amino acid residues of ACE_C and ACE_N, which might be implicated in the binding mode of the chloride ions Cl1 and Cl2. The nearest distances between atoms of the chloride ligands and the enzyme residues are also indicated. For the residues implicated in the binding of Cl1, we can observe the R186/H164 alteration and for the Cl2 the M223/W201. Very close to the binding groove of Cl2 the differentiation V518/T496 between ACE_C and ACE_N can also be observed.

In Table II, the non-conserved amino acids of ACE_C and the equivalent of ACE_N, which might be implicated in the binding of lisinopril, are indicated. The residues with common interactions with the chloride ion and lisinopril (substrate) are W279 for Cl1 and R522 for Cl2 (conserved in both domains, see Table I). Figure 2 illustrates the binding site of Cl2 in the case of ACE_C (white) and ACE_N (grey) (ACE_N numbering first), with amino acid differences of ACE_N indicated

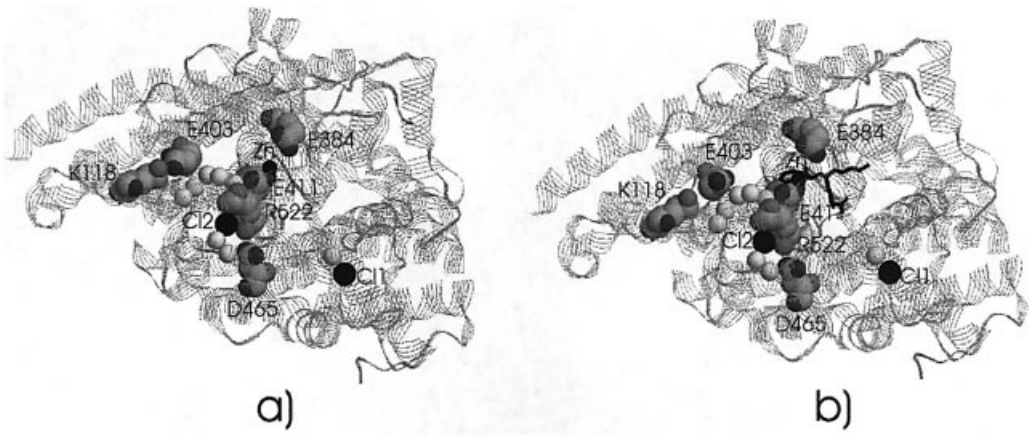

Fig. 3. Water channel network in the native ACE_C (**a**) and the lisinopril–ACE_C complex (**b**). Water molecules are shown as white spheres and the chloride ions Cl1 and Cl2 and zinc as black spheres. The amino acids R522, D465, E384 (catalytic), E403, E411 and K118 are also indicated. The ligand lisinopril in the complex is shown in black.

with asterisks. In the ACE_C–lisinopril complex, which could provide a model for the transition state of the peptide hydrolysis mechanism, the distance of the side chain of R522 (NH1) and E411 (OE) is 4.6 Å and that of Cl2 to R522 (NE) is 3.1 Å.

In an effort to investigate the chloride channel that connects the external solution with the inner part of the protein, we searched for cavities in the enzyme with CASTp (Liang *et al*., 1998). A cavity filled with a network of five water molecules (764, 767, 720, 1124, 1150) hydrogen bonded within each other is conserved in both the native and the ACE_C–lisinopril complex (Figure 3). This water network could provide a potent pore for the entrance of the Cl2 anion from the solution and an indication of mechanistically implicated water molecules (see discussion below). The water molecule that is closer to the inner part of the enzyme is located 5.8 Å from the zinc cation and ~6 Å from the Cl2 anion.

In *Salmonella enterica* serovar *typhimurium* CLC Cl^- channels, four separate highly conserved regions, named the selectivity filter, are brought together near the ion-binding site. These regions include the sequences GSGIP (106–110), G(K/R)EGP (146–150) and GXFXP (355–359), in addition to Y445. It is significant that these sequences occur at the N termini of α-helices (Dutzler *et al*., 2002), which creates an electrostatically favourable environment for anion binding, because of the N-terminal positive helix dipole. Interestingly, common chloride binding motifs could be found in both ACE_C and ACE_N sequences. The location of the A, B, C regions and Y445 of the StCLC channel and the relevant regions of the ACE_C chloride binding channel (A, 401–410; B, 456–465; C, 516–526) and Y224 are shown in Figure 4A. In the case of the StCLC channel, Cl^- does not make direct contact with a positive charge (arginine and/or lysine) and is stabilized instead with partial positive charges contributed by α-helix dipole interactions and by contacts with main-chain and side-chain nitrogen and oxygen groups (Figure 4A, a). In the case of ACE_C (Figure 4A, b), the chloride ion is located at the N-terminal positive end of two dipole helices, near the C-terminal negative end of two dipole helices, and makes direct contact with a full positive charge (R522). In both cases, in addition to the interactions with polar functional groups, the Cl^- ion is surrounded by a number of hydrophobic amino acid side chains (see Table I).

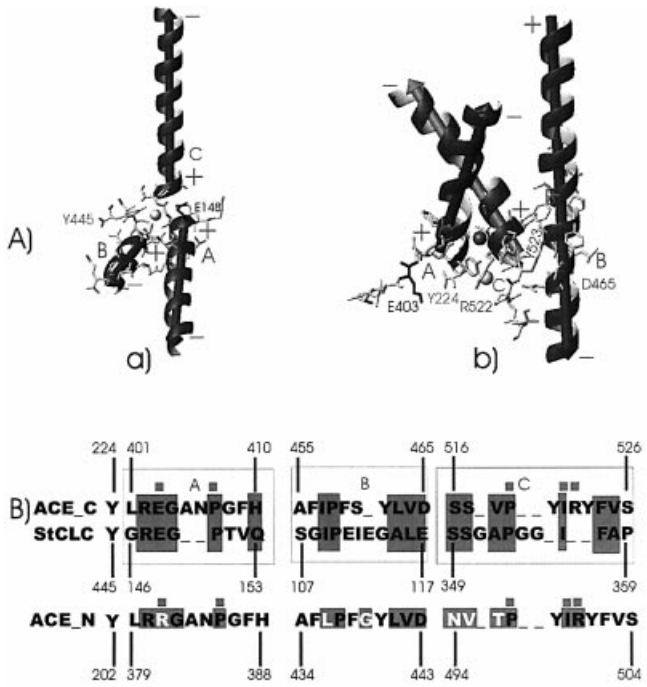

Fig. 4. (**A**) (a) Helix dipoles, denoted with arrows, of the Cl^- selectivity filter residues (A, B, C) for the StCLC channel (*S.typhimurium* ClC) surrounding a Cl^- ion (white sphere). (b) Helix dipoles of the relevant amino acid sequence groups (A, B, C) surrounding a Cl^- ion (white sphere) in ACE_C. The zinc ion is shown in grey. (**B**) Sequence alignment of the A, B and C Cl^- selectivity filter of StClC channel with potent residues of the ACE_C, which are shown in grey boxes. In the lower trace, alignment with the ACE_N is shown; amino acid differences with ACE_C are shown in white and amino acids of ACE_C and ACE_N in contact with Cl^- are indicated with grey squares.

In the ion conduction pathway of the StCLC Cl^- channel, the carboxylate group of E148 (Figure 4A, a) is sandwiched between the positive ends of two α-helices and possibly blocks Cl^- permeation. Dutzler *et al.* proposed that Cl^- opens the gate and binds to the anion-selective region by dislodging the glutamate side chain (Dutzler *et al*., 2002). In ACE_C, E403 is in the similar conserved motif of the A ion selectivity filter and is positioned in the positive end of an α-helix (Figure 4A, b).

Hence for E403 of ACE_C, a similar role could be proposed to that of E148 of the StCLC Cl^- channel, during the Cl^- permeation.

In the 'anion selectivity filter' B, a highly conserved aspartate group, D465/443 of ACE_C and ACE_N, respectively, is located. In the same position a glutamate ion (E117) is present in the anion selectivity filter of StCLC (Figure 4B). Further, the side chain of D465 of ACE_C (D443 ACE_N) points to a water molecule that is directly hydrogen bonded to another water molecule belonging to the first shell of the coordination sphere of Cl2 (Figure 3). Interestingly, R522 of ACE_C is located in a helix that is tilted pointing to the chloride ion. This perturbation from the rest axis could be due to P519 (proline kink). It could be suggested that R522 acts as a carrier of the neighbouring Y523 and forms a salt bridge with D465 in the absence of chloride ion. In this case, Y523 is away from the zinc-binding site and, thus, cannot stabilize the substrate–enzyme transition state. Constructively, the requirement for a negative anion that could serve as the counterpart of R522 is obvious. As can be seen in Figures 2 and 4, Cl2 attracts R522 away from D465. Thus, Cl2 plays the role of an ionic switch. Upon chloride binding, activation of the mechanism could be accomplished through the breaking of this salt bridge, resulting in a movement of Y523 towards the active site.

How do these new structural findings relate to previous mutational data? In angiotensin I hydrolysis assays, removal of Cl^- from both the N- and C-domains results in a reversible inactivation (Liu *et al*., 2001); however, the N-domain active site is fully activated at relatively low chloride ion concentration (Jaspard *et al*., 1993). Mutations of R1098 (R522 in *t*ACE) with Q in ACE_C and R500 with Q in ACE_N result in a loss of the Cl^- dependence (Liu *et al*., 2001) and peptide hydrolysis is similar to that obtained with the optimum chloride ion concentration. As previously emphasized, E403 of ACE_C plays a similar role to that of E148 of the StCLC Cl^- channel, during the Cl^- permeation. A possible interaction of E403, which is facing the entrance of the water-channel network (Figure 3a and b), with the side chain of R522 would result in blocking of the water network channel. Thus, access of Cl^- counter ions is required to dislodge the side chain of E403 and open the gate. In the same position where E403 is located in ACE_C, R381 is present in the floor of the channel of the substrate-binding groove of ACE_N (Figure 4B), which alleviates the requirement for high chloride ion concentration. Interestingly, the side chain of E403 alternates its side chain orientation upon lisinopril binding, in the native structure of the enzyme $\chi1$, –70.6°; $\chi2$, 115.8°; $\chi3$, –52.8°, the distance R522(NH1)–E403(OE2) is 9.20 Å and in the complex, $\chi1$, –59.9°; $\chi2$, –67.3°; $\chi3$, –8.0°, and the distance R522(NH1)–E403(OE1) is 7.90 Å. Furthermore, the K154 to E154 mutant in rabbit testicular ACE (Sen *et al*., 1993) and modification of the relative K694 of rabbit lung ACE (Chen *et al*., 1990), which correspond to K118 of ACE_C, exhibited drastically reduced chloride sensitivity. The side chain of K118 in the native form of the enzyme forms a salt bridge with the side chain of E403 [the distance K118 (NZ)–E403 (OE2) is 2.8 Å] that is not conserved in the lisinopril–ACE complex (this distance becomes 5.13 Å). Breaking of the salt bridge in the mutant presumably reduces a potent interaction of E403 with R522. Interestingly, in the same position that K118 is located in ACE_C, A94 is located in ACE_N, which results in a lower chloride demand for catalytic activity of the N-domain.

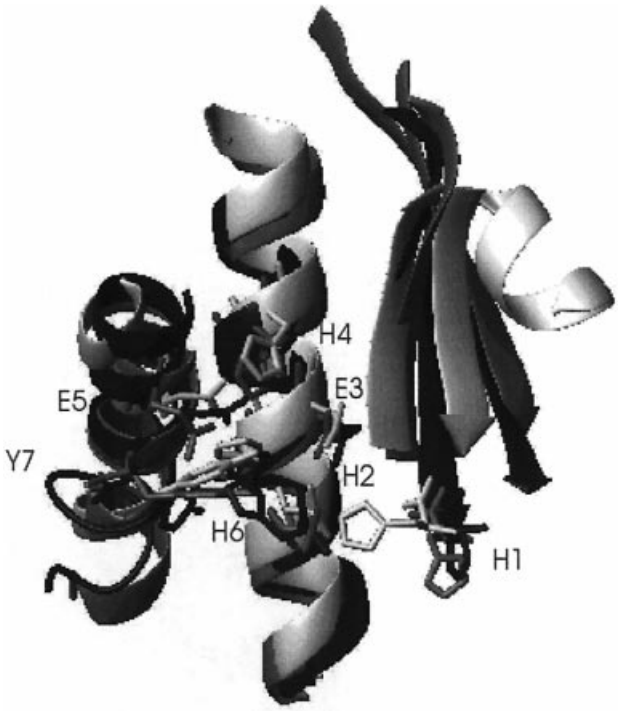

Fig. 5. Structural comparison of the active site of ACE (white) with neurolysin (light grey) and *P.furiosus* (black). H1, H331/353/425/238; H2, H361/383/474/269; E3, E362/384/475/270; H4, H365/387/478/273; E5, E389/411/503/299; H6, H491/513/601/411; Y7, Y501/523/613/423, with ACE_N numbering first, ACE_C second, neurolysin third and *P.furiosus* carboxypeptidase last.

Structural comparison of ACE_C and ACE_N with the endopeptidases neprilysin and neurolysin and P.furiosus carboxypeptidase—proposition for a common catalytic mechanism

Superposition of ACE_C with the endopeptidase neprilysin, which hydrolyses also angiotensin I (Deddish *et al*., 1998), indicates very high structure homology in the peptide-binding groove, despite the low overall structural and amino acid homology (supplementary Figure S4). In neprilysin, H711, which has been reported to play a role in the stabilization of the transition state enzyme–substrate complex (Dion *et al*., 1993; Oefner *et al*., 2000), is superimposed with Y523 of ACE_C, suggesting a similar functional role. In neprilysin, H711 is located in the extrapolation of the parallel helix (helix II, supplementary Figure S4) in a flexible loop. In ACE_C, Y523 is located in helix I (supplementary Figure S4), where the anion binding R522 of ACE_C is located and is tilted pointing to the chloride ion. This kink of helix I from the rest axis, located near P519, could be facilitated upon chloride binding owing to rearrangement of Y523 towards the stabilization of the transition state complex. This finding further supports the proposition that R522, in the absence of chloride binding, could form a salt bridge with D465 (the distance between R522 and D465 is expected to be reduced in the case that helix I is not perturbed from the rest axis, as for the parallel helix II of neprilysin).

Structure homology searches revealed significant homology of ACE with *Rattus norvegicus* neurolysin (PDB i.d.: 1I1I) (Brown *et al*., 2001), a zinc-dependent endopeptidase, and *P.furiosus* carboxypeptidase (PDB i.d.: 1KA2) (Arndt *et al*.,

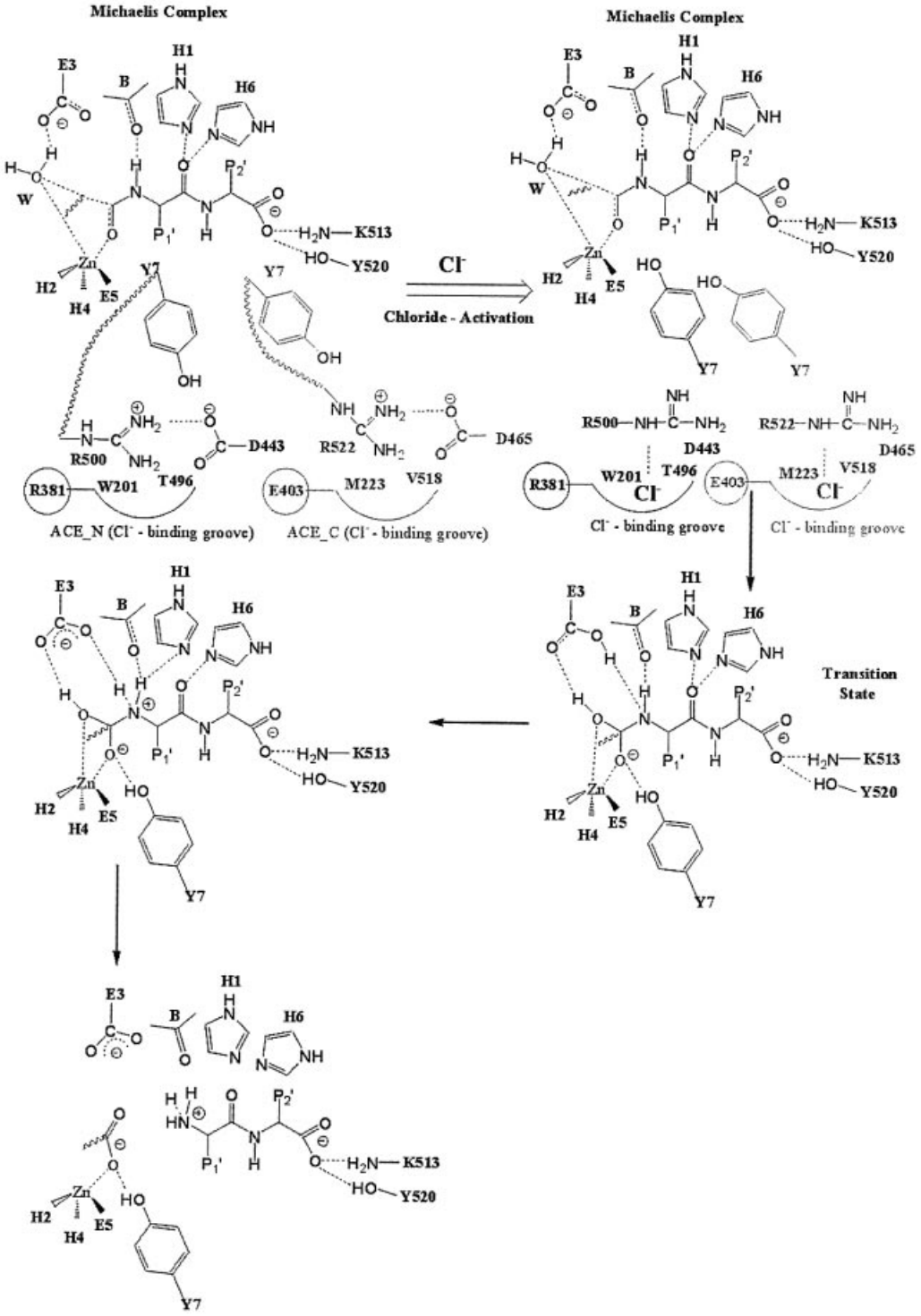

Fig. 6. Schematic diagram of a possible catalytic mechanism for peptide binding and hydrolysis of ACE_C, ACE_N, neurolysin and *P.furiosus* carboxypeptidase. The first step (in grey) denotes the chloride activation mechanism for ACE_C. R500 in ACE_N and R522 in ACE_C are the 'carriers' of the transition state stabilizing Y7. The definition of H1, H2, E3, H4, E5, H6 and Y7 (amino acid residues involved in the catalytic mechanism of the four proteins) is denoted in Figure 5. B stands for a bulky apolar group (see text).

2002). Neurolysin is a member of the M3 family of oligopeptidases, which cleaves neurotensin, a 13-residue neuropeptide between residues 10 and 11 and *P.furiosus* carboxypeptidase is a member of the M32 family of carboxypeptidases. The three enzymes, in addition to neprilysin, possess the HEXXH active-site motif and consist of an abundance of α-helices with very few β-sheets. Superposition of *P.furiosus* carboxypeptidase and neurolysin with ACE_C(N) results in an r.m.s.d. of 3.11 Å for 399 Cα atoms and 3.4 Å for 361 Cα atoms, respectively, thus resembling a closer fold to *P.furiosus* carboxypeptidase. Superposition of the active sites of ACE_C with *P.furiosus* carboxypeptidase and neurolysin

results in an r.m.s.d. of 1.45 Å for 108 Cα atoms and 1.56 Å for 128 Cα atoms, respectively.

A structure alignment is provided in Figure 5, whereas the structure-based sequence alignment is illustrated in supplementary Figure S4. Neurolysin (681 residues) is larger than ACE_C (625 residues), ACE_N (630 residues) and *P.furiosus* carboxypeptidase (499 residues) and has a number of extra structural elements. One of the major differences between the structures is the β-sheet near the active site, which is composed of five strands in neurolysin, two strands in ACE_C(N) and three strands in *P.furiosus* carboxypeptidase. In the light of this structural similarity, it may be suggested that the aforementioned enzymes are evolved from a common ancestor by divergent evolution.

Despite this high structural similarity, the amino acid identity between ACE_C and ACE_N with neurolysin is only 10%; with *P.furiosus* carboxypeptidase the sequence alignment is 16 and 14% for ACE_N and ACE_C, respectively, based on the amino acids used in the structure superposition. A BLAST search showed no sequence similarity between these two domains (Madden *et al*., 1996), emphasizing the high sequence diversity among these proteins. Using the structure alignment, we identified 16 conserved residues among the four enzymes with the following seven residues proposed to play an important role in catalysis (ACE_N/ACE_C/neurolysin/*P.furiosus* carboxypeptidase): H331/353/425/238; H361/383/474/269; E362/384/475/270; H365/387/478/273; E389/411/503/299; H491/513/601/411; Y501/523/613/423 (Figure 5).

The mechanism of cleavage of AI by ACE is unclear at present. A fundamental issue is the orientation of the substrate, which could be addressed from the structure of the *t*ACE–lisinopril complex that could provide a model of the transition state hydrolysis mechanism. All HEXXH proteins reported to date have a similar binding pocket around the active site, which implies that the substrate binding has a similar orientation relative to the HEXXH motif. Indeed, the ACE zinc ligands H2 (H361/383) and H4 (H365/387) of the HEXXH motif and E5 (E389/411) of the conserved HEAI signature sequence adopt conformations similar to those found in other HEXXH-containing proteases.

A general base-type mechanism for ACE_C and ACE_N, which is similar to other HEXXH proteins (Hangauer *et al*., 1984; Matthews, 1988), could be proposed for these enzymes (Figure 6). Zinc serves to stabilize a bound water/hydroxide and/or to activate the scissile carbonyl of the substrate by serving as a Lewis acid. The active site glutamate, E3 (E362/384) of the HEXXH motif, assists in the nucleophilic attack of the activated water/hydroxide on the carbonyl to form a tetrahedral intermediate, by acting as a general acid/base that can shuttle the hydrogen atom from the activated water to the scissile amide nitrogen of the substrate. Protonation of this amide nitrogen makes it a better leaving group, thereby facilitating cleavage of the amide bond.

H1 (H331/353) and A332/354 (B) of the HAS signature sequence in ACE_N and ACE_C, (HPF and HAA in *P.furiosus* and neurolisin, respectively), may play a role in orienting the amide nitrogen to accept this hydrogen and in stabilizing the proper transition state. The carbonyl oxygen of A332/354 on strand β-4 could form a hydrogen bond with the scissile NH of the substrate, which facilitates the protonation by the proton shuttle E3, as in other HEXXH metalloproteases (Holden *et al*., 1987; Holden and Matthews, 1988; Grams *et al*., 1996; Chan *et al*., 1997). Upon protonation, H1 (H331/353) could play a role in transition state stabilization, as a hydrogen bond acceptor that would stabilize the tetrahedral transition state. H1 (H331/353) is conserved in all members of the ACE family, as well as in neurolysin and *P.furiosus* carboxypeptidase (Figure S4; see also the sequence alignment in Figure S5 in the supplementary material). Consistent with such a role, N112 in thermolysin is suggested to play a similar role and is located at nearly the same position (Holden *et al*., 1987; Holden and Matthews, 1988). H6 (H491/513) could also play a significant role in the stabilization of the transition state through the formation of a hydrogen bond with the carbonyl group of the P1′ position, since mutation to alanine resulted in a reduction of the catalytic activity of *s*ACE (Fernandez *et al*., 2001).

Y7 (Y501/523) is another residue that could play a crucial role in stabilizing the tetrahedral intermediate and further as a determinative step discriminating ACE_C and ACE_N with regard to the role of the chloride ion. This residue is conserved for the entire family of ACE in addition to neurolysin (Y613; Figure 5 and supplementary Figure S5) and *P.furiosus* carboxypeptidase (Y423; Figure 5 and supplementary Figure S5) and is located at a similar position in the active site as residues Y149, H231 and H711 of astacin, thermolysin and neprilysin, respectively. These residues have been suggested to stabilize the negative charge of the oxyanion intermediate by hydrogen bonding one of the coordinating zinc oxygens (Holden *et al*., 1987; Holden and Matthews, 1988; Grams *et al*., 1996), as is also shown in the X-ray structure of the 'transition state' ACE_C–lisinopril complex. As has been discussed above, in the absence of chloride ion in ACE_C, R522 could possibly interact with D465 and move Y7 (Y523) away from the catalytic center (Figure 6). The presence of the chloride ions induces the stabilization of the transition state through Y7 (Y523), by locking R522 away from D465. The resulting tetrahedral intermediate subsequently decomposes to yield the products.

Conclusions

A homology-model reconstruction of the ACE_N domain, based on the known X-ray structure of *t*ACE that represents the C- catalytic domain of the somatic isoform of human *s*ACE, offers detailed insights into the structural–functional features discriminating the two catalytic domains. The roles of the two chloride ions, unmasked from the X-ray structure, were assigned, suggesting the first one to be responsible for the stabilization of the substrate in the binding groove. The second chloride ion is a mechanistically significant binding ion, which could break the salt bridge between R522/500 and D465/443 and facilitate the movement of Y523/501 of ACE_C/ACE_N towards the active site. A potent pore for the entrance of the Cl2 anion from the solution was also identified. Structure-based sequence alignment of ACE_C and ACE_N with the endopeptidases neprilysin and neurolysin, and *P.furiosus* carboxypeptidase revealed common key residues important for the peptide hydrolysis mechanism and stabilization of the transition state. The predicted model has been found to be consistent with several mutational and substrate hydrolysis data.

Rationalization of the functional differences of the two domains of ACE (ACE_C and ACE_N) might also provide a basis for the design of enzyme model systems (Galanis *et al*., 2003) and of domain-selective ACE inhibitors with an improved pharmacological profile in terms of stability,

duration of action and selectivity in the treatment of cardiovascular and renal diseases.

References

Araujo,M.C., Melo,R.L., Cesari,M.H., Juliano,M.A., Juliano,L. and Carmona,A.K. (2000) *Biochemistry*, **39**, 8519–8525.

Arndt,J.W., Hao,B., Ramakrishnan,V., Cheng,T., Chan,S.I. and Chan,M.K. (2002) *Structure (Camb.)*, **10**, 215–224.

Azizi,M., Rousseau,A., Ezan,E., Guyene,T.T., Michelet,S., Grognet,J.M., Lenfant,M., Corvol,P. and Menard,J. (1996) *J. Clin. Invest.*, **97**, 839–844.

Bairoch,A. and Apweiler,R. (2000) *Nucleic Acids Res.* **28**, 45–48.

Baudin,B. and Beneteau-Burnat,B. (1999) *J. Enzyme Inhib.*, **14**, 447–456.

Berman,H.M., Westbrook,J., Feng,Z., Gilliland,G., Bhat,T.N., Weissig,H., Shindyalov,I.N. and Bourne,P.E. (2000) *Nucleic Acids Res.*, **28**, 235–242.

Brown,C.K., Madauss,K., Lian,W., Beck,M.R., Tolbert,W.D. and Rodgers,D.W. (2001) *Proc. Natl Acad. Sci. USA*, **98**, 3127–3132.

Bunning,P. and Riordan,J.F. (1983) *Biochemistry*, **22**, 110–116.

Chan,M.K., Gong,W., Rajagopalan,P.T., Hao,B., Tsai,C.M. and Pei,D. (1997) *Biochemistry*, **36**, 13904–13909.

Chen,Y.N. and Riordan,J.F. (1990) *Biochemistry*, **29**, 10493–10498.

Chen,Y.N., Ehlers,M.R. and Riordan,J.F. (1992) *Biochem. Biophys. Res. Commun.*, **184**, 306–309.

Chubb,A.J., Schwager,S.L., Woodman,Z.L., Ehlers,M.R. and Sturrock,E.D. (2002) *Biochem. Biophys. Res. Commun.*, **297**, 1225–1230.

Coates,D., Isaac,R.E., Cotton,J., Siviter,R., Williams,T.A., Shirras,A., Corvol,P. and Dive,V. (2000) *Biochemistry*, **39**, 8963–8969.

Colovos,C. and Yeates,T.O. (1993) *Protein Sci.*, **2**, 1511–1519.

Corvol,P. and Williams,T.A. (1996) In Barrett,A.J., Rawlings,N.D. and Woessner,J.F. (eds), *Handbook of Proteolytic Enzymes*. Academic Press, New York, pp. 1066–1076.

Corvol,P., Williams,T.A. and Soubrier,F. (1995) *Methods Enzymol.*, **248**, 283–305.

Cotton,J., Hayashi,M.A., Cuniasse,P., Vazeux,G., Ianzer,D., De Camargo,A.C. and Dive,V. (2002) *Biochemistry*, **41**, 6065–6071.

Deddish,P.A., Wang,L.-X., Jackman,H.L., Michel,B., Wang,J., Skidgel,R.A. and Erdos,E.G. (1996) *J. Pharmacol. Exp. Ther.*, **279**, 1582–1589.

Deddish,P.A., Marcic,B., Jackman,H.L., Wang,H.Z., Skidgel,R.A. and Erdos,E.G. (1998) *Hypertension*, **31**, 912–917.

Dion,N., Le Moual,H., Crine,P. and Boileau,G. (1993) *FEBS Lett.*, **318**, 301–304.

Dive,V., Cotton,J., Yiotakis,A., Michaud,A., Vassiliou,S., Jiracek,J., Vazeux,G., Chauvet,M.T., Cuniasse,P. and Corvol,P. (1999) *Proc. Natl Acad. Sci. USA*, **96**, 4330–4335.

Donoghue,M. *et al*. (2000) *Circ. Res.*, **87**, 1–9.

Dutzler,R., Campbell,E.B., Cadene,M., Chait,B.T. and MacKinnon,R. (2002) *Nature*, **415**, 287–294.

Ehlers,M.R. and Riordan,J.F. (1991) *Biochemistry*, **30**, 7118–7126.

Erdos,E.G. (1990) *Hypertension*, **16**, 363–370.

Fernandez,M., Liu,X., Wouters,M.A., Heyberger,S. and Husain,A. (2001) *J. Biol. Chem.*, **276**, 4998–5004.

Galanis,A., Spyroulias,G., Pierattelli,R., Tzakos,A., Troganis,A., Gerothanassis,I., Pairas,G., Manessi-Zoupa,E. and Cordopatis,P. (2003) *Biopolymers*, **69**, 244–252.

Georgiadis,D., Beau,F., Czarny,B., Cotton,J., Yiotakis,A. and Dive,V. (2003) *Circ. Res.*, **93**, 148–154.

Gibrat,J.F., Madej,T. and Bryant,S.H. (1996) *Curr. Opin. Struct. Biol.*, **6**, 377–385.

Goli,U. and Galardy,R. (1986) *Biochemistry*, **25**, 7136–7142.

Grams,F., Dive,V., Yiotakis,A., Yiallouros,I., Vassiliou,S., Zwilling,R., Bode,W. and Stocker,W. (1996) *Nat. Struct. Biol.*, **3**, 671–675.

Grinstein,S., Nikolskaya,I., Klyachko,N., Levashov,A. and Kost,O. (1999) *Biochemistry (Mosc.)*, **64**, 571–580.

Grinstein,S., Levashov,A. and Kost,O. (2001) *Biochemistry (Mosc.)*, **66**, 34–41.

Hagaman,J.R., Moyer,J.S., Bachman,E.S., Sibony,M., Magyar,P.L., Welch,J.E., Smithies,O., Krege,J.H. and O'Brien,D.A. (1998) *Proc. Natl Acad. Sci. USA*, **95**, 2552–2557.

Hangauer,D.G., Monzingo,A.F. and Matthews,B.W. (1984) *Biochemistry*, **23**, 5730–5741.

He,Q.Y., Mason,A.B., Nguyen,V., MacGillivray,R.T. and Woodworth,R.C. (2000) *Biochem. J.*, **350**, 909–915.

Holden,H.M. and Matthews,B.W. (1988) *J. Biol. Chem.*, **263**, 3256–3260.

Holden,H.M., Tronrud,D.E., Monzingo,A.F., Weaver,L.H. and Matthews,B.W. (1987) *Biochemistry*, **26**, 8542–8553.

Holm,L. and Sander,C. (1993) *J. Mol. Biol.*, **233**, 123–138.

Holm,L. and Sander,C. (1996) *Methods Enzymol.*, **266**, 653–662.

Hooper,N.M. (1991) *Int. J. Biochem.*, **23**, 641–647.

Hooper,N.M. (1994) *FEBS Lett.*, **354**, 1–6.

Hubert,C., Houot,A.M., Corvol,P. and Soubrier,F. (1991) *J. Biol. Chem.*, **266**, 15377–15383.

Jaspard,E., Wei,L. and Alhenc-Gelas,F. (1993) *J. Biol. Chem.*, **268**, 9496–9503.

Kim,H.M., Shin,D.R., Yoo,O.J., Lee,H. and Lee,J.O. (2003) *FEBS Lett.*, **538**, 65–70.

Koradi,R., Billeter,M. and Wuthrich,K. (1996) *J. Mol. Graph.*, **14**, 51–55.

Kost,O., Orth,T., Nikolskaya,I., Nametkin,S. and Levashov,A. (1994) *Biochemistry (Mosc.)*, **59**, 1301–1306.

Kost,O., Orth,T., Nikolskaya,I., Nametkin,S. and Levashov,A. (1998) *Biochem. Mol. Biol. Int.*, **44**, 535–542.

Kost,O., Balyasnikova,I., Chemodanova,E., Nikolskaya,I., Albrecht,R. and Danilov,S. (2003) *Biochemistry*, **42**, 6965–6976.

Laskowski,R.A., MacArthur,M.W., Moss,D.S. and Thornton,J.M. (1993) *J. Appl. Crystallogr.*, **26**, 283–291.

Liang,J., Edelsbrunner,H. and Woodward,C. (1998) *Protein Sci.*, **7**, 1884–1897.

Liu,X., Fernandez,M., Wouters,M.A., Heyberger,S. and Husain,A. (2001) *J. Biol. Chem.*, **276**, 33518–33525.

Luthy,R., Bowie,J.U. and Eisenberg,D. (1992) *Nature*, **356**, 83–85.

Madden,T.L., Tatusov,R.L. and Zhang,J. (1996) *Methods Enzymol.*, **266**, 131–141.

Matthews,B.W. (1988) *Acc. Chem. Res.*, **21**, 333–340.

Michaud,A., Williams,A., Chauvet,T. and Corvol,P. (1997) *Mol. Pharmacol.*, **51**, 1070–1076.

Michaud,A., Chauvet,M.T. and Corvol,P. (1999) *Biochem. Pharmacol.*, **57**, 611–618.

Murzin,A.G., Brenner,S.E., Hubbard,T. and Chothia,C. (1995) *J. Mol. Biol.*, **247**, 536–540.

Natesh,R., Schwager,S.L., Sturrock,E.D. and Acharya,K.R. (2003) *Nature*, **421**, 551–554.

Oefner,C., D'Arcy,A., Hennig,M., Winkler,F.K. and Dale,G.E. (2000) *J. Mol. Biol.*, **296**, 341–349.

Orengo,C.A., Michie,A.D., Jones,S., Jones,D.T., Swindells,M.B. and Thornton,J.M. (1997) *Structure*, **5**, 1093–1108.

Perich,R.B., Jackson,B. and Johnston,C.I. (1994) *Eur. J. Pharmacol.*, **266**, 201–211.

Rieger,K.J., Saez-Servent,N., Papet,M.P., Wdzieczak-Bakala,J., Morgat,J.L., Thierry,J., Voelter,W. and Lenfant,M. (1993) *Biochem. J.*, **296**, 373–378.

Rohrbach,M.S., Williams,E.B.,Jr and Rolstad,R.A. (1981) *J. Biol. Chem.*, **256**, 225–230.

Rousseau,A., Michaud,A., Chauvet,M.T., Lenfant,M. and Corvol,P. (1995) *J. Biol. Chem.*, **270**, 3656–3661.

Sali,A., Potterton,L., Yuan,F., van Vlijmen,H. and Karplus,M. (1995) *Proteins*, **23**, 318–326.

Schechter,I. and Berger,A. (1967) *Biochem. Biophys. Res. Commun.*, **27**, 157–162.

Scrutton,N.S. and Raine,A.R. (1996) *Biochem. J.*, **319**, 1–8.

Sen,I., Kasturi,S., Abdul Jabbar,M. and Sen,G.C. (1993) *J. Biol. Chem.*, **268**, 25748–25754.

Shapiro,R., Holmquist,B. and Riordan,J.F. (1983) *Biochemistry*, **22**, 3850–3857.

Sippl,M.J. (1993) *Proteins*, **17**, 355–362.

Skidgel,R.A. and Erdos,E.G. (1985) *Proc. Natl Acad. Sci. USA*, **82**, 1025–1029.

Soubrier,F., Alhenc-Gelas,F., Hubert,C., Allegrini,J., John,M., Tregear,G. and Corvol,P. (1988) *Proc. Natl Acad. Sci. USA*, **85**, 9386–9390.

Soubrier,F., Hubert,C., Testut,P., Nadaud,S., Alhenc-Gelas,F. and Corvol,P. (1993a) *J. Hypertens.*, **11**, 471–476.

Soubrier,F., Wei,L., Hubert,C., Clauser,E., Alhenc-Gelas,F. and Corvol,P. (1993b) *J. Hypertens.*, **11**, 599–604.

Sturrock,E.D., Yu,X.C., Wu,Z., Biemann,K. and Riordan,J.F. (1996) *Biochemistry*, **35**, 9560–9566.

Taylor,C.A., Coates,D. and Shirras,A.D. (1996) *Gene*, **181**, 191–197.

Thiele,R., Zimmer,R. and Lengauer,T. (1999) *J. Mol. Biol.*, **290**, 757–779.

Thompson,J.D., Higgins,D.G. and Gibson,T.J. (1994) *Nucleic Acids Res.*, **22**, 4673–4680.

Thompson,J.D., Plewniak,F., Thierry,J. and Poch,O. (2000) *Nucleic Acids Res.*, **28**, 2919–2926.

Tipnis,S.R., Hooper,N.M., Hyde,R., Karran,E., Christie,G. and Turner,A.J. (2000) *J. Biol. Chem.*, **275**, 33238–33243.

Tzakos,A., Bonvin,A., Troganis,A., Cordopatis,P., Amzel,M., Gerothanassis,I.P. and van Nuland,N. (2003) *Eur. J. Biochem.*, **270**, 849–860.

Tzakos,A., Troganis,A. and Gerothanassis,I.P., (2004) *Curr. Top. Med. Chem.*, **4**, in press.
Ucar,G. and Ozer,I. (1992) *Biochem. Pharmacol.*, **44**, 565–570.
Wei,L., Alhenc-Gelas,F., Corvol,P. and Clauser,E. (1991) *J. Biol. Chem.*, **266**, 9002–9008.
Wei,L., Clauser,E., Alhenc-Gelas,F. and Corvol,P. (1992) *J. Biol. Chem.*, **267**, 13398–13405.
Williams,T.A., Corvol,P. and Soubrier,F. (1994) *J. Biol. Chem.*, **269**, 29430–29434.

Received May 23, 2003; revised October 16, 2003; accepted October 21, 2003